RevMexAA (Serie de Conferencias), **3**, 61–68 (1995)

MHD TURBULENCE, CLOUD FORMATION, AND STAR FORMATION IN THE ISM

Enrique Vázquez-Semadeni,
Instituto de Astronomía, UNAM, Apdo. Postal 70-264, 04510 México D.F., México
Thierry Passot and Annick Pouquet
Observatoire de Nice, BP 229, 06340 Nice CEDEX 4, France

RESUMEN

Discutimos el papel de la turbulencia en la formación de nubes y estrellas, según se observa en simulaciones numéricas del medio interestelar. La compresión turbulenta en las interfases entre corrientes de gas en colisión es responsable de la formación de nubes de tamaño intermedio ($\lesssim 100$ pc) y pequeñas (algunas decenas de pc), aunque las más pequeñas también se pueden formar por la fragmentación de cáscaras en expansión alrededor de centros de calentamiento por estrellas. Los más grandes complejos de nubes (varios cientos de pc) parecen formarse por un lento proceso de fusión de nubes individuales promovido por la inestabilidad gravitacional. Este proceso se puede describir como una tendencia hacia la homogeneización del medio a gran escala debida a la gravedad, más que como colisiones entre nubes. Estos mecanismos operan también en presencia del campo magnético y de la rotación, aunque con ligeras variaciones en la compresibilidad del flujo y la morfología de las nubes que dependen de la intensidad y topología del campo. En resumen, el papel de la turbulencia parece ser doble: los modos turbulentos pequeños contribuyen al soporte de las nubes contra su autogravedad, mientras que los modos grandes pueden tanto formar como destruir nubes.

ABSTRACT

We discuss the role of turbulence in cloud and star formation, as observed in numerical simulations of the interstellar medium. Turbulent compression at the interfaces of colliding gas streams is responsible for the formation of intermediate ($\lesssim 100$ pc) and small clouds (a few tens of pc), although the smallest clouds can also form from fragmentation of expanding shells around stellar heating centers. The largest cloud complexes (several hundred pc) seem to form by slow, gravitational instability-driven merging of individual clouds, which can actually be described as a large-scale tendency towards homogenization of the flow due to gravity rather than cloud collisions. These mechanisms operate as well in the presence of a magnetic field and rotation, although slight variations in the compressibility and cloud morphology are present which depend on the strength and topology of the field. In summary, the role of turbulence in the life cycle of clouds appears to be twofold: small-scale modes contribute to cloud support, while large-scale modes can both form and disrupt clouds.

Key words: **ISM: CLOUDS – ISM: MAGNETIC FIELDS – ISM: STRUCTURE – INSTABILITIES – TURBULENCE**

1. INTRODUCTION

The interstellar medium (ISM) is a highly compressible turbulent flow (e.g., Dickman 1985; Scalo 1987; Falgarone 1989) in which turbulent density fluctuations are likely to be ubiquitous. With a few exceptions, however, most treatments of cloud dynamics and formation that include turbulence have traditionally considered only the contribution of small-scale turbulent motions for cloud support against gravitational collapse (e.g., Chandrasekhar 1951; Shu, Adams, & Lizano 1987; Bonazzola et al. 1987; Léorat, Passot, & Pouquet 1990; Elmegreen 1991; Vázquez-Semadeni & Gazol 1995). Actually, turbulent motions at cloud scales or larger may have both cloud-forming and disrupting effects, which may be respectively associated with the compressive and shearing modes of the turbulence. Although early contentions were that, being supersonic, turbulent motions should dissipate rapidly (e.g., Goldreich & Kwan 1974), later studies suggested that the energy sources present in the Galaxy (mainly stellar activity and galactic differential rotation) could be enough to replenish the turbulence (e.g., Fleck 1980; see the review by Dickman 1985). Stellar energy injection originates mostly from OB winds and supernova (SN) explosions, and the average rates for the Galaxy have been determined observationally by a number of authors (e.g., Abbott 1982; Van Buren 1989).

Cloud and star formation (hereafter CF and SF, respectively) at the interfaces between colliding flow streams has been discussed analytically by Hunter & Fleck (1982) and Elmegreen (1993). Low-resolution hydrodynamical simulations of colliding flow streams were performed by Hunter et al. (1986), and the effects of stellar forcing in the large-scale flow have been simulated by Bania & Lyon (1980), Chiang & Prendergast (1985), Chiang & Bregman (1988) and Rosen, Bregman, & Norman (1993). Fully turbulent regimes in the vertical direction in the galactic disk have been explored by Rosen et al. (1993) and by Rosen & Bregman (1995). However, all of these calculations have omitted self-gravity and magnetic fields, and have employed somewhat unrealistic SF schemes, thus rendering it impossible to discuss the full energy budget and the life cycles of the clouds that form.

In this paper we discuss the interplay between turbulence, CF, and SF in our recent numerical simulations of the ISM. The simulations incorporate stellar and diffuse heating with a more realistic SF scheme, parameterized cooling, self-gravity and large-scale shear (Vázquez-Semadeni, Passot, & Pouquet 1995, hereafter Paper I), and magnetic fields and rotation (Passot, Vázquez-Semadeni, & Pouquet 1995, hereafter Paper II). In §2 we briefly describe the model system, in §§3 and 4 we discuss results without and with magnetic fields, and in §5 we summarize the main conclusions.

2. THE MODEL

In the numerical calculations we consider a square region of the ISM, one kpc on a side, in the galactic plane. The hydrodynamic equations are solved in two dimensions using a pseudospectral scheme with periodic boundary conditions. Model terms are included for the diffuse and stellar heating and the parameterized cooling. Additionally, a large-scale sinusoidal shear profile is imposed on the flow. In cases with rotation and magnetic fields, the Coriolis and Lorentz forces are added to the momentum equation, together with the induction equation. In all cases, Poisson's equation for the gravitational potential arising from the density *fluctuations* is also solved. Fiducial values of all parameters used correspond to realistic values for the ISM, within the uncertainties reported in the literature. Details on the numerical scheme can be found in Papers I and II.

All variables are normalized to values that can be considered typical of the ISM at a scale of one kpc. Thus, the units of density, temperature and velocity are respectively $\rho_o = 1$ cm^{-3}, $T_o = 10^4$ K and $u_o = 11.7$ km s^{-1}. Note that u_o is chosen equal to the adiabatic sound speed at T_o.

Stellar heating is modeled as a local heating center a few pixels across; it is turned on when the local value of the density exceeds a threshold ρ_c and $\nabla \cdot \mathbf{u} < 0$ locally, and turned off after a time equal to the typical lifetime of OB stars ($\sim 5 \times 10^6$ yr). This mimics the heating from ionizing radiation from massive stars. The diffuse heating is taken to be proportional to $\rho^{-\alpha}$, with $0 < \alpha < 1$, mimicking the self-shielding of clouds against background UV radiation. Finally, radiative cooling is parameterized as a term $\rho\Lambda$, where Λ is a piecewise power law of the temperature with exponent β_i in the i-th temperature interval, of the kind introduced by Chiang & Bregman (1988).

In magnetic runs, the total magnetic field is split into a constant, uniform azimuthal component $\mathbf{B}_o$ and a fluctuating component $\mathbf{B}_{rms}$.

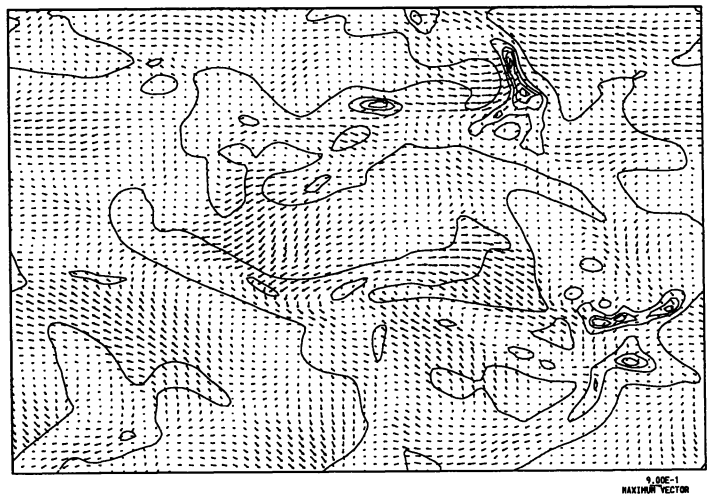

Fig. 1. Contour plot of the density field with superimposed vector velocity field for a 512 × 512 non-magnetic run, at $t = 8 \times 10^7$ yr into the evolution. Note that clouds are mostly located at the interfaces between colliding flow streams.

3. NON-MAGNETIC RESULTS

One of the most immediate results from the simulations using the fiducial parameter values is that the thermal (heating and cooling) time scales are much shorter than the dynamical (eddy turnover) time scales, a result already pointed out by Elmegreen (1993). This has the interesting consequence that diffuse heating and radiative cooling are almost always in equilibrium with each other (except at sites of SF, where the dominant form of heating is stellar), and thus the temperature becomes exclusively a function of the density. In turn, the ideal gas equation of state determines the thermal pressure, which then becomes a function of the density as well, exhibiting a nearly polytropic behavior. Indeed, it is shown in Papers I and II that, far from SF sites, the temperature and thermal pressure are given by

$$T_{\rm eq} = \left[\frac{\Gamma_{\rm o}\rho_{\rm IC}^{\alpha}}{\Lambda_i \rho^{1+\alpha}}\right]^{1/\beta_i} \qquad P_{\rm eq} = \frac{\rho T_{\rm eq}}{\gamma} = \frac{\rho^{\gamma_{\rm eff}}}{\gamma}\left[\frac{\Gamma_{\rm o}\rho_{\rm IC}^{\alpha}}{\Lambda_i}\right]^{1/\beta_i},$$

where $\gamma = 5/3$ is the ratio of specific heats for the gas, $\rho_{\rm IC} \sim 0.2$ is a typical value of the density in the intercloud medium (ICM), $\Gamma_{\rm o}$ is the diffuse heating rate at $\rho = \rho_{\rm IC}$, Λ_i is the coefficient of the cooling function in the i-th temperature interval, and $\gamma_{\rm eff} = 1 - (1+\alpha)/\beta_i$ is an effective polytropic exponent. For the chosen values of α and β_i, $\gamma_{\rm eff}$ is smaller than 0.5 below $T = 10^5$ K. This implies that the flow is highly compressible and, for practical purposes, the temperature and thermal pressure can thus be taken as being *enslaved* by the density field, which is in turn controlled by the velocity field.

In the simulations, expanding bubbles around SF sites ("H II regions") are the only very-high-pressure regions and do not follow the above equilibrium relations. However, by the time their heating "stars" turn off, they have reached sizes of only a few tens of pc, and the shells they produce continue to move inertially and rapidly merge with the general turbulent flow. Therefore, although the smallest clouds form from the disrupted shells, larger clouds basically constitute the turbulent density fluctuations in the flow, arising mostly where larger-scale gas streams collide (Figure 1). This result is in agreement with earlier speculations by Hunter & Fleck (1982) and Elmegreen (1993).

The largest clouds in the simulations (several hundred pc) appear to form by a combined effect of turbulence and gravity. Intermediate-sized clouds appear to merge to form the largest complexes. However, these "mergers" do not constitute "cloud collisions" in the usual sense, as the process is rather smooth and only noticeable when comparing epochs separated by several 10^7 yr. In fact, this effect can be thought of more as a large-scale homogenization of the flow by gravity, as exemplified in Figures 2a and 2b (see also the video accompanying Paper I). This effect is not observed in runs with reduced or zero gravity, in which, in fact, the star formation

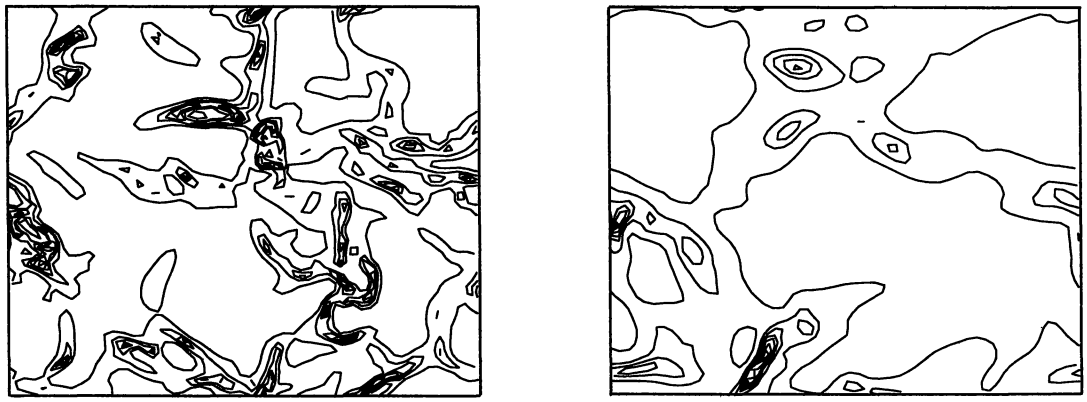

Fig. 2. Contour plots of the density field for the same run as in Fig. 1, a) (left) at a) $t = 3.9 \times 10^7$ and b) (right) at $t = 15.1 \times 10^7$, showing the trend towards homogenization at late times, apparently induced by gravity.

rate (SFR) decays rapidly to zero. The importance of gravity for large cloud formation is particularly interesting because the initial choice of parameters ($\langle T \rangle = 10^4$ K, $\langle \rho \rangle = 1$ cm^{-3}) for the simulations is such that the Jeans length is $L_J = (\pi c^2/G\rho_o)^{1/2} \sim 2$ kpc — twice the size of the integration domain at $t = 0$. However, we note that the initial conditions are out of equilibrium; the turbulent velocity dispersion in the domain is ~ 6 km s^{-1} and the system cools very rapidly to $\langle T \rangle \sim 6,000$ K. Furthermore, a gravitational instability analysis considering the effective barotropic behavior given by eq. (1b) (Paper II) gives an effective Jeans length

$$L_{\rm eff} = \left[\frac{\gamma_{\rm eff}\pi c^2}{\gamma G\rho_o}\right]^{1/2} \sim \text{ 0.8–1.1 kpc,}$$

for $\gamma_{\rm eff} \sim 0.5$. Here, c is taken as the sound speed corresponding to the mean temperature in the simulations (including the ICM). Note that this value of c is typically slightly larger than the rms turbulent velocity dispersion in the domain. Thus, the domain can be effectively gravitationally unstable after $t = 0$. This issue was not explicitly stated in Paper I, although it was speculated that self-gravity was responsible for the formation of the largest clouds in the simulations.

Note that intermediate clouds that form from turbulent density fluctuations can also become gravitationally unstable, as suggested by the simulations in Paper II, which cover a range including lower values of $\gamma_{\rm eff}$. In fact, simulations in which SF is not allowed (Vázquez-Semadeni & Mendoza, 1995), exhibit collapse of intermediate-scale clouds generated by turbulent fluctuations. Thus, SF itself prevents further generalized collapse of gravitationally unstable clouds as it generates more turbulence (Franco & Cox 1983). This mechanism may be at the origin of the low efficiency of SF in the ISM (see, e.g., Evans 1991). Finally, note that clouds in the simulations have strong internal velocity fluctuations arising either from the turbulent velocities that formed them and/or from the turbulence generated by SF. Quiescent, bullet-like clouds do not exist in our simulations, as also pointed out for real clouds by Falgarone & Pérault (1988).

Concerning the efficiency of energy injection by the stars, it was estimated in Paper I that ~ 0.05 % of the energy injected by stars ends up as turbulent kinetic energy of the flow. Under these conditions, a self-sustaining cycle sets in, in which turbulence induces SF through density fluctuations, and in turn, SF feeds the turbulence. Unfortunately, these results cannot be considered conclusive evidence that stellar energy injection is sufficient to maintain the global turbulence, since the stability of the cycle depends on the adjustable parameter ρ_c. However, realistic massive-star formation rates are observed in the model ($\sim 10^{-4}$ OB stars kpc^{-2} yr^{-1}), suggesting that the result is feasible.

In summary, three mechanisms of cloud formation appear to be dominant in the simulations: intermediate-scale clouds form mainly by turbulent density fluctuations at the interfaces of colliding gas streams; small-

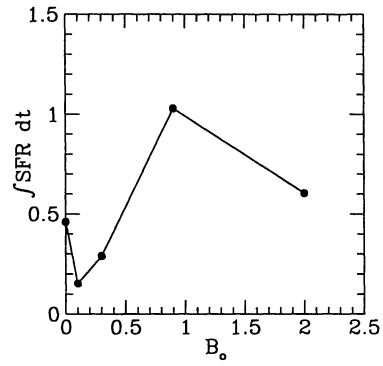

Fig. 3. Time integral of the star formation rate for various runs as a function of the initial value of the uniform component of the magnetic field B_o. At small B_o, SF is inhibited because B_o is small enough not to counteract magnetic braking, but is able to prevent radial collapse of sheared condensations. Intermediate values of B_o counteract magnetic braking and thus promote SF. Very large values of B_o inhibit SF because the magnetic field makes the medium more rigid.

scale clouds can form by either the same mechanism or from fragmentation of expanding shells around SF sites. Finally, the largest cloud complexes form through turbulent merging of intermediate clouds, driven by gravitational instability. Thus, the role of turbulence in the life cycle of clouds appears to be twofold: small-scale (with respect to the cloud's size) turbulent modes contribute to cloud support, while large-scale modes provide either cloud-forming or cloud-disrupting mechanisms. However, an important caveat must be mentioned here: the simulations clearly do not have turbulent modes at scales larger than the largest clouds. The effects of these modes on the kpc-sized clouds is thus not represented, even though they could drastically affect the conclusions based on small-scale turbulence. In that context, simulations of the entire galactic disk would be necessary.

4. MAGNETIC EFFECTS

4.1. Effects of the Magnetic Field on Cloud and Star Formation

A linear instability analysis for the galactic disk including an azimuthal magnetic field has been carried out by Elmegreen (1991, 1994). The corresponding analysis for the two-dimensional system of our simulations is given in Paper II. In the absence of shear, a weak magnetic field stabilizes the medium by opposing collapse of radial perturbations, while a strong field is destabilizing by preventing Coriolis spin-up of azimuthal perturbations (magnetic braking). Since realistic perturbations should have both radial and azimuthal components, the shear-less magnetic case is always unstable. In the presence of sufficiently strong shear, the field becomes stabilizing again, as azimuthal perturbations are sheared into the radial direction before they have time to collapse.

In the turbulent regime, the cloud formation mechanisms described for the non-magnetic cases continue to hold, although somewhat modified by the magnetic field by criteria similar to those obtained from the instability analysis. Indeed, in Paper II it was found that fully turbulent simulations exhibit varying degrees of compressibility and SF as the initial uniform azimuthal component of the field B_o is increased. This effect is shown in Figure 3, which gives the time-integral of the SFR for various runs with progressively higher values of B_o. Moderate values are seen to decrease the overall SFR, while larger values are seen to increase it. Interestingly, saturation at very large B_o appears to occur, which can be interpreted as a global "rigidization" of the medium by the field. In fact, "H II regions" in the simulations do not expand nearly as much in the presence of B_o as they do in non-magnetic cases. This "pressure cooker" effect is similar to the results of Slavin & Cox (1993) for the expansion of SN remnants in the presence of magnetic fields. In fact, in the simulations, this cloud-confining effect of the magnetic field is as notorious as its cloud-supporting effect.

An unexpected effect of the uniform field component is that clouds appear to be slightly *more roundish and less filamentary* at larger values of B_o (Figure 4), contrary to the common belief that the opposite effect should occur. We speculate that this phenomenon is due to a combination of factors: first, the above mentioned

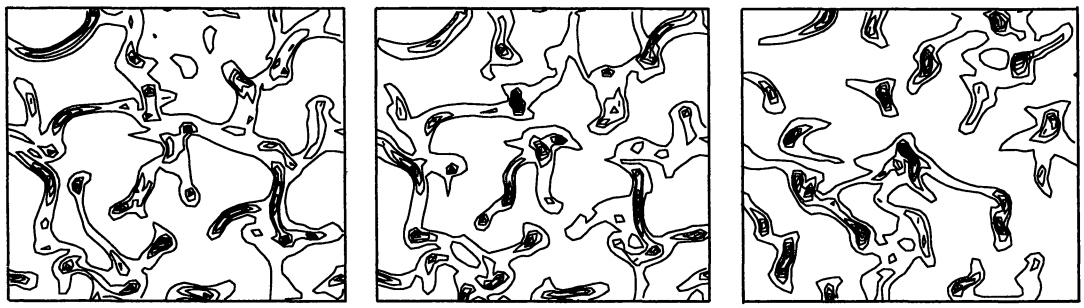

Fig. 4. Contour plots of the density field at $t = 5.2 \times 10^6$ yr for three runs with $B_o = 0, 1.5$ and 10 μG (left to right), but otherwise identical. Note the tendency towards more roundish structures as B_o increases.

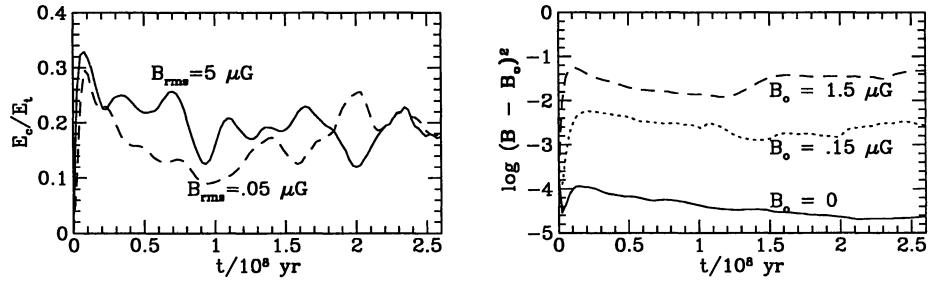

Fig. 5. a) (left) Evolution of the ratio of compressible to total kinetic energy for two runs with different initial values of the fluctuating component of the field. The characteristic scale of the initial fluctuations is 1/4 the size of the integration box. Initially the run with stronger fluctuations has larger compressibility. Due to the inverse magnetic cascade and stellar activity, however, by $t \sim 1.5 \times 10^8$ yr the fluctuating magnetic energies of the two runs are comparable, causing comparable compressibilities. b) (right) Evolution of the fluctuating component of the magnetic energy for three runs with different initial values of the uniform component of the field. Both the amplitude of the fluctuations and their time derivative are seen to increase with B_o.

"pressure cooker" effect which does not allow shells to expand very much; second, gas motions along field lines (when promoted by compressions as opposed to body forces like gravity), cause an increase in the field component perpendicular to the motion, thus opposing it.

The effects of a uniform azimuthal field are to be contrasted to those of an initial small-scale fluctuating field $B_{\rm rms}$. In this case, magnetic tension in the field lines induces small scale compressions in the flow, increasing the global compressibility (Figure 5a) of the medium.

4.2. Effects of Star Formation on the Magnetic Field

Because stellar heating is the ultimate source of energy for the turbulence in the simulations, it has important affects on the magnitude and topology of the magnetic field as well. One of the most important results is that SF appears to be capable of maintaining and even increasing the total magnetic energy in the flow by means of the compressible, non-periodic forcing it exerts. This result is all the more interesting considering that the simulations are two-dimensional, and therefore cannot support dynamo activity.

The mechanism apparently responsible for the magnetic amplification in our simulations requires the presence of the uniform component of the field B_o (Paper II). This is exemplified in Figure 5b, which shows the evolution of the fluctuating magnetic energy for three runs with different values of B_o. Clearly, both the amplitude of the fluctuations and their time derivative are larger at larger B_o.

An interesting feature of the dynamics in the simulations is that there seems to be no single predominant physical agent. Inasmuch as the field constrains fluid and cloud motions to some extent, the field is in turn

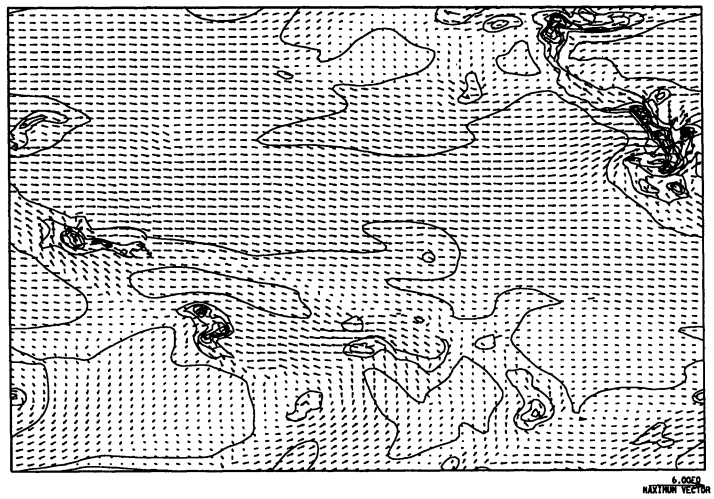

Fig. 6. Density and magnetic fields for a 512×512 run at $t = 0.42 \times 10^8$ yr. Note the strong magnetic turbulence inside clouds and the rather smooth character of the magnetic field in the ICM. Regions of alignment of the magnetic field and density features can be seen, for example, in the filament in the upper right corner. However there are also regions where the magnetic field is perpendicular to the density features such as the lower portion of the same cloud and also the cloud near the center of the lower left quadrant.

strongly distorted by the turbulence and SF. In particular, in clouds formed by turbulent compressions, the field exhibits a tendency towards alignment with elongated density features, as the field component perpendicular to the compression is amplified by flux freezing. This mechanism has the further consequence that the field is generally larger inside clouds than in the ICM by factors of ~ 4 ($\sim 3\mu$G for the ICM and $\sim 12\mu$G within clouds), with excursions up to factors ~ 10. Also, the strong turbulence within the clouds causes the field to have strong internal fluctuations (Figure 6).

It is noteworthy that the stellar energy injection occurs at scales small compared with the size of the system, and thus kinetic and magnetic energy transfer to larger scales is observed. Although observed here in a two-dimensional context, it is known that in three dimensions an inverse cascade of magnetic helicity exists (as opposed to a square magnetic potential in two dimensions), with the magnetic energy following to a lesser extent (Pouquet, Frisch, & Léorat, 1976; Meneguzzi, Frisch, & Pouquet, 1981; Horiuchi & Sato, 1986, 1988). It will be of great interest to determine whether the observed cascades are still maintained in three-dimensional simulations with forcing at the small scales.

5. CONCLUSIONS

Turbulence is a major cloud-forming agent in numerical simulations of the ISM at the kpc scale (Papers I and II). The non-magnetic simulations (Paper I) suggest that intermediate ($\lesssim 100$ pc) and small (a few tens of pc) clouds mainly form at the interfaces of colliding flow streams. The smallest clouds can additionally form from fragmentation of expanding shells around stellar heating centers. Large cloud complexes (several hundred pc) appear to form from gravitational instability. However, since the medium is turbulent and contains already sizable clouds, the formation of the large complexes proceeds through gradual merging of the clouds that is almost imperceptible as one watches the simulation evolve, but is noticeable when comparing epochs separated by several 10^7 yr.

SF injects energy into the turbulence, and the simulations indicate that a self-sustaining cycle may be established, although the caveat exists that the simulations contain an adjustable parameter, namely the threshold density for SF ρ_c, which controls the stability of the cycle.

The magnetic field introduces quantitative variations in these mechanisms, but does not seem to alter them essentially, although the role of the Parker instability cannot be evaluated by the simulations, as they neglect the vertical direction in the Galaxy. The field modulates the density contrast that can be achieved by turbulent compressions, as well as the morphology of the clouds. In turn, the turbulent magnetic energy is also

fed by stellar activity, provided a sizable uniform component of the field is present. The stellar energy injection occurs at comparatively small scales, and energy cascades to larger scales. Whether this is an artifact of the two-dimensionality of the simulations remains to be evaluated by resorting to three-dimensional computations.

In summary, the role of turbulence in the life cycle of clouds appears to be twofold: small-scale modes contribute to cloud support, while large-scale modes can both form or disrupt clouds.

Finally, it should be pointed out that the simulations so far have not included the energy injection from supernovae or OB winds, which can inject energy at significantly larger rates than heating from ionizing radiation of main sequence OB stars. The largest turbulent velocity dispersion that can be imparted to the flow by stellar heating is comparable to the thermal velocity dispersion at the temperature of our "H II regions", $\sim 10^4$ K, which roughly balances gravity for these complexes. In the non-magnetic case, this turbulent energy is enough to blow the complexes apart, but not in the magnetic case because of the "pressure cooker" effect. The inclusion of SN/wind energy should cause these clouds to be easily disrupted. Work in this direction is in progress (Gazol et al. 1995).

REFERENCES

Abbott, D. C. 1982, ApJ 263, 723
Bania, T. M., & Lyon, J. G. 1980, ApJ, 239, 173
Bonazzola, S., Falgarone, E., Heyvaerts, J., Pérault, M., Puget, J. L. 1987, A&A 172, 293
Chandrasekhar, S. 1951, Proc. R. Soc. London, 210, 26
Chiang, W.-H., & Bregman, J. N. 1988, ApJ, 328, 427
Chiang, W.-H., & Prendergast, K. H. 1985, ApJ, 297, 507
Dickman, R. L. 1985, in Protostars and Planets II, ed. D. C. Black & M. S. Matthews (Tucson: Univ. of Arizona Press), 150
Elmegreen, B. G. 1991, ApJ, 378, 139
———. 1993, ApJ, 419, L29
———. 1994, ApJ, 433, 39
Evans, N. J., 1991, in Frontiers in Stellar Evolution, ed. D. L. Lambert (San Francisco: A. S. P.), 45
Falgarone, E. 1989, in IAU Colloquium 120, Structure and Dynamics of the Interstellar Medium, ed. G. Tenorio-Tagle, M. Moles, & J. Melnick (Berlin: SpringerVerlag), 68
Falgarone, E., & Pérault, M. 1988, A&A, 205, L1
Fleck, R. C., Jr. 1980, ApJ, 242, 1019
Franco, J., & Cox, D.P. 1983, ApJ, 273, 243.
Gazol, A., Passot, T., Pouquet, A., & Vázquez-Semadeni, E. 1995, in preparation
Goldreich, P., & Kwan, J. 1974, ApJ, 189, 441
Horiuchi, R., & Sato, T. 1986, Phys. Fluids 26, 1161
———. 1988, Phys. Fluids 31, 1142
Hunter, J. H., Jr., & Fleck, R. C. 1982, ApJ, 256, 505
Hunter, J. H., Jr., Sandford, M. T. II, Whitaker, R. W., & Klein, R. I. 1986, ApJ, 305, 309
Léorat, J., Passot, T., & Pouquet, A. 1990, MNRAS, 243, 293
Meneguzzi, M., Frisch, U., & Pouquet, A. 1981, Phys. Rev. Lett. 47, 1060
Passot, T., Vázquez-Semadeni, E., & Pouquet, A. 1995, ApJ, submitted (Paper II)
Pouquet, A., Frisch, U., & Léorat, J. 1976, J. Fluid Mech., 77, 321
Rosen, A., & Bregman, J. N. 1995, ApJ, 440, 634
Rosen, A., Bregman, J. N., & Norman, M. L. 1993, ApJ, 413, 137
Scalo, J. M. 1987, in Interstellar Processes, ed. D. J. Hollenbach & H. A. Thronson (Dordrecht: Reidel), 349
Shu, F. N., Adams, F. C., & Lizano, S. 1987, ARA&A, 25, 23
Slavin, J., & Cox, D. 1993, ApJ, 417, 187
Van Buren, D. 1989, ApJ, 338, 147
Vázquez-Semadeni, E., & Gazol, A. 1995, A&A, in press
Vázquez-Semadeni, E., Passot, T., & Pouquet, A. 1995, ApJ, 441, 702 (Paper I)
Vázquez-Semadeni, E., & Mendoza, V. 1995, in preparation